On the mass segregation of stars and brown dwarfs in Taurus

Richard J. Parker,[1,2]★ Jerome Bouvier,[3] Simon P. Goodwin,[2] Estelle Moraux,[3] Richard J. Allison,[2] Sylvain Guieu[4] and Manuel Güdel[5]

[1]*Institute for Astronomy, ETH Zürich, Wolfgang-Pauli-Strasse 27, 8093 Zürich, Switzerland*
[2]*Department of Physics and Astronomy, University of Sheffield, Sheffield S3 7RH*
[3]*Laboratoire d'Astrophysique de Grenoble, Observatoire de Grenoble, BP 53, 38041 Grenoble Cedex 9, France*
[4]*European Southern Observatory, Alonso de Cordova 3107, Vitacura, Santiago, Chile*
[5]*Department of Astronomy, University of Vienna, Türkenschanzstraße 17, Vienna A-1180, Austria*

ABSTRACT

We use the new minimum spanning tree (MST) method to look for mass segregation in the Taurus association. The method computes the ratio of MST lengths of any chosen subset of objects, including the most massive stars and brown dwarfs, to the MST lengths of random sets of stars and brown dwarfs in the cluster. This mass segregation ratio (Λ_{MSR}) enables a quantitative measure of the spatial distribution of high- and low-mass stars, and brown dwarfs to be made in Taurus.

We find that the most massive stars in Taurus are *inversely mass segregated* with $\Lambda_{MSR} = 0.70 \pm 0.10$ ($\Lambda_{MSR} = 1$ corresponds to no mass segregation), which differs from the strong mass segregation signatures found in more dense and massive clusters such as Orion. The brown dwarfs in Taurus are not mass segregated, although we find evidence that some low-mass stars are, with an $\Lambda_{MSR} = 1.25 \pm 0.15$. Finally, we compare our results to previous measures of the spatial distribution of stars and brown dwarfs in Taurus, and briefly discuss their implications.

Key words: methods: data analysis – brown dwarfs – stars: low-mass – galaxies: star clusters: individual: Taurus.

1 INTRODUCTION

The Taurus association is a nearby young cluster (at 140 pc with an age of ~ 1 Myr; Kenyon, Dobrzycka & Hartmann 1994) still in the process of forming stars from its natal molecular cloud. It contains relatively few stars (<400) of which most are contained within several main aggregates (e.g. Gomez et al. 1993; Kenyon, Gómez & Whitney 2008). Star formation in Taurus appears to be occurring along three parallel filaments with the central filament coincident with the main region of aggregates (e.g. Ungerechts & Thaddeus 1987).

Taurus has a spatial extent of ~ 30 pc (Palla & Stahler 2002) and has a low number density compared with, for example, the Orion nebula cluster. Due to its sparse environment and young age, it is thought that very little dynamical evolution has taken place (Kroupa & Bouvier 2003), and the observed stars are direct signatures of the star formation process in this region (Luhman 2006). For this reason, attempts have been made to quantify the spatial distribution of stars and brown dwarfs in Taurus to test various formation hypotheses

including those that postulate a different formation scenario for brown dwarfs over stars (e.g. Reipurth & Clarke 2001; Thies & Kroupa 2007).

In this paper, we use the new minimum spanning tree (MST) method (Allison et al. 2009) to look for differences in the distribution of low- and high-mass objects in Taurus. We describe the observational sample used in Section 2 before presenting the results in Section 3. In Section 4, we compare the MST method to other measures of spatial distribution in Taurus, we discuss our results in Section 5 and present our conclusions in Section 6.

This is the first in a series of papers in which we will discuss the formation of stars and brown dwarfs in Taurus by considering the process from pre-stellar cores to the subsequent effects of dynamical evolution on the cluster population.

2 THE OBSERVATIONAL SAMPLE

Our primary data base for the following analysis is a catalogue of 442 Taurus sources compiled by the XMM-Newton Extended Survey of the Taurus Molecular Cloud (XEST) collaboration (Güdel et al. 2007) as an 'input catalogue' for the XEST project. This input catalogue was compiled by cross-identifying objects between

★ E-mail: rparker@phys.ethz.ch

various previous catalogues of Taurus members (in particular from Kenyon & Hartmann 1995; Briceño et al. 2002; Palla & Stahler 2002) and general all-sky catalogues relevant for pre-main-sequence stars. Ancillary information, such as photometric and spectroscopic data, coordinates, masses and ages, was then extracted from the individual catalogues, although for some all-sky survey catalogues we confined the search for counterparts within a radius of 8° of the position RA (2000.0) = $4^h 25^m$, Dec. (2000.0) = 25° (note that this constraint is irrelevant for the *identification* of Taurus members which relies on previous dedicated Taurus catalogues). Information from SIMBAD and the Two Micron All Sky Survey catalogues (essentially spectral types, coordinates and photometry) was confined to the areas covered by the XEST X-ray exposures (again this does not affect the membership identification relevant for our study). A condensed version of the input catalogue for the areas covered by the XEST survey was published in Güdel et al. (2007), where the relevant catalogue bibliography is also described.

Of these 442 catalogue sources, 293 have a mass estimate derived from bolometric luminosity, L_{bol}, and effective temperature, T_{eff}, using Siess, Dufour & Forestini (2000) isochrones with a relative uncertainty of the order of 20 per cent (see Güdel et al. 2007). Of the remaining 149 objects without a mass listed in the catalogue, 55 have a known spectral type. We used this spectral type to derive a mass estimate from Siess et al. (2000) isochrones assuming an age of 2 Myr. This yielded a total of 328 Taurus members following the removal of duplicates. Binary companions were also included in the sample, where available. Of these 328 objects, 20 do not appear in the more recent compilation of Taurus members by Kenyon et al. (2008) and we therefore rejected them from the analysis. We will discuss the possible effects of hidden binaries and rogue non-members on our results in Section 3.

The XEST catalogue misses most of the recently discovered very low mass stars and substellar members of the Taurus cloud. We therefore completed the XEST sample with the low-mass end of the Taurus population taken from Kenyon et al. (2008) compilation that lists 382 Taurus members. The latter data base includes 85 very low mass Taurus members which were not included in the XEST data base. Of these, only 53 have a spectral type listed in Luhman et al. (2010). We used these spectral types to derive mass estimates from Siess et al. (2000) 2-Myr isochrone.

Adding these more recent detections to the XEST source list eventually yields a catalogue of 361 Taurus members with a mass estimate. We conservatively estimate the relative error on the mass to be of the order of 30 per cent. Alternatively, as a check to the robustness of our results below, we also used the Luhman et al. (2010) list of 324 Taurus members with known spectral types for which we derived a mass estimate using the Siess et al. (2000) 2-Myr isochrone.

We show a map of the Taurus cluster made with our data in Fig. 1. The (blue) crosses show 20 least massive objects (brown dwarfs) in the cluster, whereas the large (red) points show 20 most massive stars in the cluster. Extensive surveys of various areas of Taurus by Briceño et al. (1998, 2002), Luhman (2000), Luhman et al. (2003), Luhman (2004, 2006) and Guieu et al. (2006) are shown by the black outlines. It is thought that these areas are more or less observationally complete, whereas the regions outside of these lines may not be (Luhman et al. 2009, 2010; Monin et al. 2010).
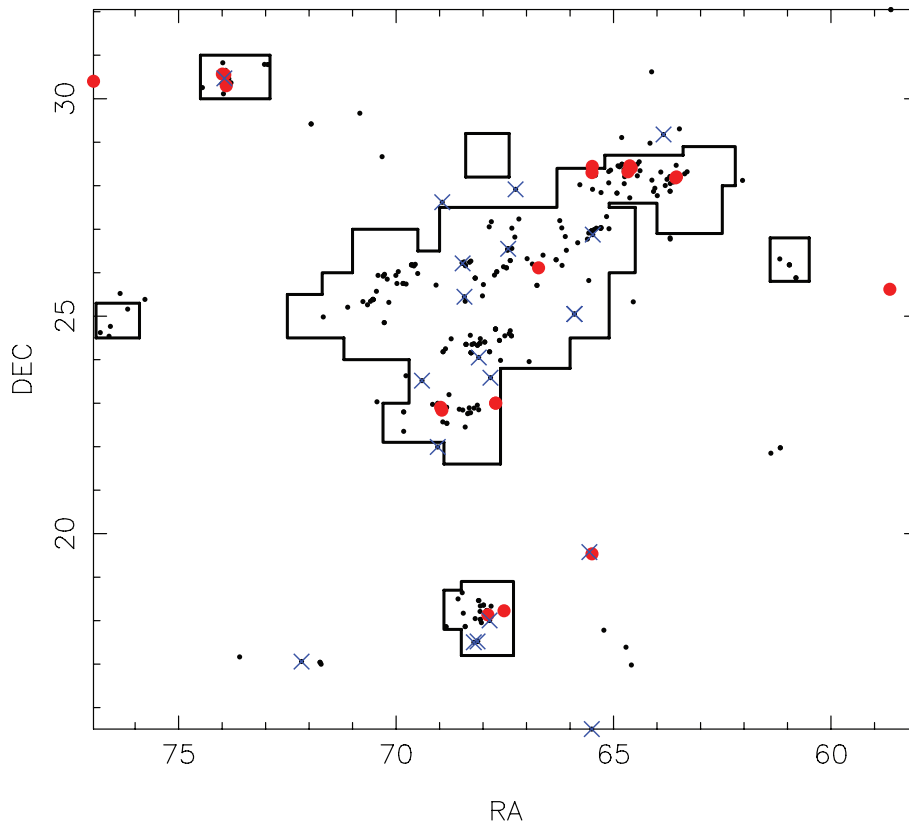

Figure 1. A map of the Taurus cluster showing the 361 objects in our data set. The 20 least massive cluster members are shown by the (blue) crosses and the 20 most massive cluster members are shown by the large (red) dots. The areas of Taurus that are observationally complete (surveys by Briceño et al. 2002; Guieu et al. 2006; Luhman 2006; Luhman et al. 2010, and references therein) are inside the solid lines.

3 RESULTS

In this section, we describe the MST method used to quantify mass segregation in clusters before applying it to sets of objects of similar mass in Taurus.

3.1 The minimum spanning tree method

Following Allison et al. (2009), we adopt the MST method to quantify the level of mass segregation in Taurus. The MST of a set of points is the path connecting all the points via the shortest possible path-length but which contains no closed loops (e.g. Prim 1957; Cartwright & Whitworth 2004).

We use the algorithm of Prim (1957) to construct MSTs in our data set. We first make an ordered list of the separations between all possible pairs of stars.[1] Stars are then connected together in 'nodes', starting with the shortest separations and proceeding through the list in order of increasing separation, forming new nodes if the formation of the node does not result in a closed loop.

3.2 Quantifying mass segregation

Observationally, 'mass segregation' is a term used to describe the central concentration of massive stars in a star cluster (the prime example probably being the Trapezium of massive stars at the centre of the Orion nebula cluster). In addition, mass segregation is often used in dynamics to refer to the central concentration of massive stars, and the wider distribution of low-mass stars caused by energy equipartition due to two-body relaxation.

In this paper, we will define 'mass segregation' in terms of the relative spatial distributions of stars in a particular mass range with respect to other stars in a cluster. This also allows us to define 'inverse mass segregation' as an underconcentration of a particular stellar mass range with respect to the other cluster members. Note that we can apply this definition to low-mass stars/brown dwarfs, and by describing a population of low-mass stars as 'inversely mass segregated', we do not mean that the high-mass stars are necessarily mass segregated.

We find the MST of the N_{MST} stars in the chosen subset and compare this to the MST of sets of N_{MST} random stars in the cluster. If the length of the MST of the chosen subset is shorter than the average length of the MSTs for the random stars, then the subset has a more concentrated distribution and is said to be mass segregated. Conversely, if the MST length of the chosen subset is longer than the average MST length, then the subset has a less concentrated distribution, and is said to be an inversely mass segregated. Alternatively, if the MST length of the chosen subset is equal to the random MST length, we can conclude that no mass segregation is present.

By taking the ratio of the average random MST length to the subset MST length, a quantitative measure of the degree of mass segregation (normal or inverse) can be obtained. We first determine the subset MST length, l_{subset}. We then determine the average length of sets of N_{MST} random stars each time, $\langle l_{average} \rangle$. There is a dispersion associated with the average length of random MSTs, which is roughly Gaussian and can be quantified as the standard deviation of the lengths $\langle l_{average} \rangle \pm \sigma_{average}$. However, we conservatively estimate the lower (upper) uncertainty as the MST length which lies 1/6 (5/6) of the way through an ordered list of all the random lengths

(corresponding to a 66 per cent deviation from the median value, $\langle l_{average} \rangle$). This determination prevents a single outlying object from heavily influencing the uncertainty. We can now define the 'mass segregation ratio' (Λ_{MSR}) as the ratio between the average random MST path-length and that of a chosen subset, or mass range of objects:

$$\Lambda_{MSR} = \frac{\langle l_{average} \rangle}{l_{subset}} {}^{+\sigma_{5/6}/l_{subset}}_{-\sigma_{1/6}/l_{subset}}. \quad (1)$$

A Λ_{MSR} of $\sim$1 shows that the stars in the chosen subset are distributed in the same way as all the other stars, whereas $\Lambda_{MSR} > 1$ indicates mass segregation and $\Lambda_{MSR} < 1$ indicates inverse mass segregation, i.e. the chosen subset is more sparsely distributed than the other stars.

As noted by Allison et al. (2009), the MST method gives a quantitative measure of mass segregation with an associated significance and it does not rely on defining the centre of a cluster (somewhat impossible for a substructured region like Taurus). It also bypasses the various binning methods used in determining the mass segregation through fitting a density profile (e.g. Adams et al. 2001; Littlefair et al. 2003) or tracing the change in mass function with radius (e.g. Gouliermis et al. 2004; Sabbi et al. 2008). We shall now apply the MST method to look for mass segregation in the high- and low-mass stellar (and substellar) populations in Taurus.

3.3 High-mass cluster members

In Fig. 1, we show the location of the 20 most massive objects in the cluster ($m \gtrsim 1.2\,M_{\odot}$) by the large (red) points. Several of them are within the central aggregates, but others are located in both the northern and southern Gomez groups (Gomez et al. 1993). In Fig. 2, we show Λ_{MSR} as a function of the number of stars in an MST for the highest mass stars. $\Lambda_{MSR} = 1$, indicating no difference between the distribution of these stars and other stars, is shown by the dashed line.

Inspection of Fig. 2 shows that the highest mass stars in the cluster are spread more widely than other stars, i.e. they are inversely mass segregated with a trough at $\Lambda_{MSR} = 0.70 \pm 0.10$.
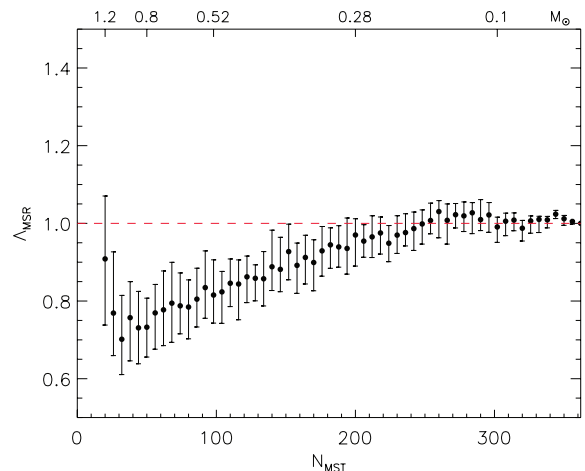

Figure 2. The evolution of the mass segregation ratio, Λ_{MSR}, with respect to the N_{MST} most massive stars in Taurus. Error bars show the 1/6th and 5/6th percentile values from the median as described in the text. The dashed line indicates $\Lambda_{MSR} = 1$, i.e. no mass segregation. We also show the lowest mass within N_{MST} stars on the top axis.

---

[1] From this point onwards, when referring, in general, to 'stars' in the cluster, we mean 'stars *and* brown dwarfs' as we are including all the objects in the observational sample.
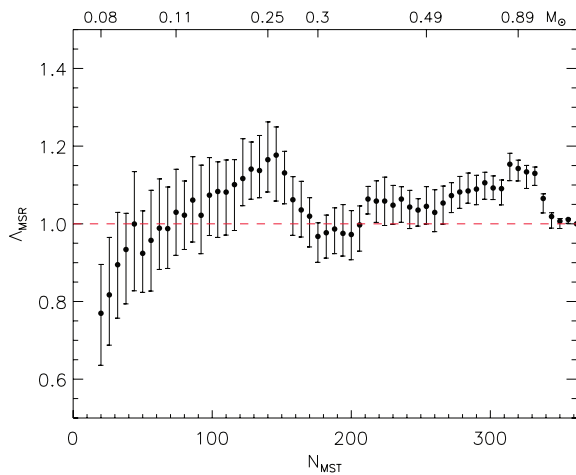
Figure 3. The evolution of the mass segregation ratio, Λ_{MSR}, with respect to the N_{MST} least massive stars (brown dwarfs) in Taurus. Error bars show the 1/6th and 5/6th percentile values from the median as described in the text. The dashed line indicates $\Lambda_{MSR} = 1$, i.e. no mass segregation. We show the highest mass within N_{MST} stars on the top axis.

3.4 Low-mass (brown dwarf) cluster members

In Fig. 1, we show the location of the 20 least massive objects (all of which are brown dwarfs) by the (blue) crosses. Most of these objects are concentrated in the central aggregates, but there are several in the outlying clumps. We also show the calculation of Λ_{MSR} as a function of the number of stars in an MST for the low-mass objects in Fig. 3 . Again $\Lambda_{MSR} = 1$, indicating no mass segregation, is shown by the dashed line.

Fig. 3 shows that the distribution of brown dwarfs in the cluster is roughly uniform, fluctuating around $\Lambda_{MSR} = 1$, with no clear trend towards either mass segregation or inverse mass segregation. There are hints that the low-intermediate-mass stars may be mass segregated (see Section 3.5), and the brown dwarfs have $\Lambda_{MSR} < 1$, but overall the plot is consistent with there being no difference between the distribution of low-mass objects and other objects.

3.5 MSTs for all cluster members

In a new variation of the MST method, we calculate the MSTs for stars as a function of mass. This is achieved by taking the MST of a subset of the N_{MST} lowest mass objects (we take the average of $N_{MST} = 40$ objects, rather than $N_{MST} = 20$, to reduce the uncertainties), and then sliding through the mass range in steps of 10 objects. For example, the first subset contains the 40 lowest mass objects, the second subset contains the 10–50 lowest mass objects, the third subset contains the 20–60 lowest mass objects and so on.[2] We then calculate Λ_{MSR} as before, and plot it in Fig. 4 as a function of the highest mass object in each subset.

It should be noted that in this method the data points are not independent of one another, with each data point including some of the same information as those in the two bins either side. However, if we move through the data set in steps of 30 objects, without any overlap, and compare the MST of each subset to random MSTs of 30 objects, the main results still hold.

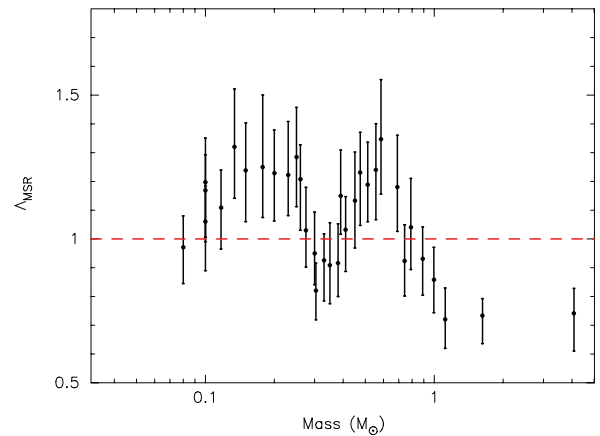[2]Because we have 361 objects in our sample, the final subset contains 41 stars rather than 40.

Figure 4. The evolution of the mass segregation ratio, Λ_{MSR}, as a function of mass for subsets of 40 stars. We plot the highest mass object in each subset. The dashed line indicates $\Lambda_{MSR} = 1$, i.e. no mass segregation.

In Fig. 4, we again see that, when compared to the MST of random subsets of objects, the brown dwarfs have a mass segregation ratio consistent with unity. Stars with masses in the range 0.1–0.25 $M_{\odot}$ appear to be slightly more concentrated (mass segregated) as do stars in the range 0.45–0.8 $M_{\odot}$. In both the mass regimes, the mass segregation ratio is $\Lambda_{MSR} = 1.25 \pm 0.15$.

Interestingly, stars with masses centred on 0.3 $M_{\odot}$ appear to have a wider distribution (slightly inversely mass segregated) with a trough at $\Lambda_{MSR} = 0.80 \pm 0.10$. In Fig. 5, we show the location of stars with mass in the range 0.25–0.35 $M_{\odot}$ by the plus signs. Most of the stars in our sample with this mass have spectral types in the range M2–M6 in the regime in which the observations may be incomplete *outside* the clumpy regions of the cluster (Guieu et al. 2006; Luhman 2006).

Our result implies that if there is a deficiency of M2–M6 objects, then those that are missing should be located within the clumps, assuming that the anomalous Λ_{MSR} around 0.3 $M_{\odot}$ is a real
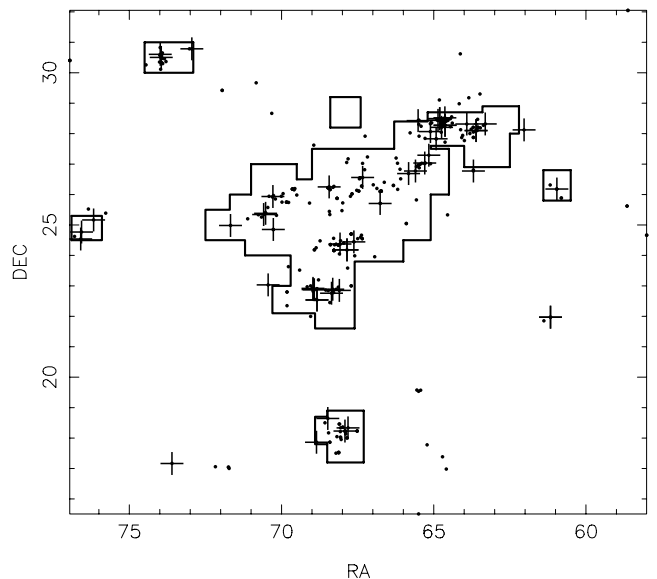

Figure 5. A map of the Taurus cluster with the positions of stars of mass 0.25–0.35 $M_{\odot}$ shown by the plus signs. The deep fields surveyed by Briceño et al. (2002), Luhman (2006), Guieu et al. (2006) and references therein are inside the solid lines.

feature, and these objects do not form via a different mechanism to e.g. objects of mass 0.2 and 0.5 M$_\odot$.

Above a mass of $\sim$0.9 M$_\odot$, the stars in each subset are inversely mass segregated with respect to random stars in the cluster confirming the results shown in Fig. 2. The level of inverse mass segregation reaches a minimum value of $\Lambda_{MSR} = 0.70 \pm 0.10$. Whilst this can be said to be a rather modest level of inverse mass segregation, it is markedly different to the MSR for stars with masses of $\sim$0.5 M$_\odot$.

3.6 Potential uncertainties

In this section, we briefly discuss the caveats associated with our results, namely the main observational uncertainties that would affect the resultant Λ_{MSR} values.

3.6.1 Mass determination

The mass determinations for most objects in our observational sample are likely to be uncertain by up to 30 per cent. It is not possible to directly quantify this in the determination of Λ_{MSR}, as this value is obtained by calculating path-lengths between objects, and is not weighted by the object's mass.[3] In order to estimate the effect of the mass uncertainty on our result, we randomly added or subtracted up to 30 per cent of the mass from each object, and then performed our analysis on these data. From multiple realizations of this experiment, we find no significant difference to the main result that the most massive stars are inversely mass segregated, and the low-mass stars are slightly mass segregated. However, the inverse mass segregation of objects at 0.3 M$_\odot$ is largely erased each time due to the addition of random noise to the mass of each star. The effect of this process is to place the stars that show strong segregation into different bins, diluting the result.

3.6.2 Binary companions

We include objects that were listed as binary systems in the catalogue of Güdel et al. (2007) in our analysis. In order to test for the effects of close or hidden binaries that may be missing from our data, we performed two experiments on the data. First, if an object was multiple, we removed it and its companion(s) from the data set altogether. This does not alter the results in any way. Secondly, we summed the masses of the components and added these to the primary, thereby accounting for (and probably overestimating) the effects of hidden companions on the mass. Again, negligible differences to the main results were found.

3.6.3 Rogue cluster members

By comparing the XEST catalogue of Güdel et al. (2007) with that of Kenyon et al. (2008), we are confident that there are no non-members masquerading in our data set. However, should there be any rogue members in our sample, they will affect the analysis in two dimensions only, i.e. background/foreground field stars will not cause an MST length to be overly long in the third dimension. Field stars in the diffuse regions (outside of the black outline in Fig. 1) could adversely affect the results, but we suggest that the chances of this are minimal for two reasons. First, the MST results

[3]An advantage of the MST method is that it does not require an absolute mass determination. One can use e.g. absolute magnitude (Sana et al. 2010).

are identical whether we include or exclude the 20 members of our sample not found in the catalogue of Kenyon et al. (2008). Secondly, using the largely independent sample from Luhman et al. (2010), we also find very similar MST results (see Section 4). This suggests that our observational sample would have to change drastically (and that there would have to be a significant number of rogue stars distributed differently to the cluster members) before the MST results are adversely compromised.

3.6.4 Missing B-type stars

The initial mass function (IMF) in Taurus has been the subject of much debate. Initially, it was thought that Taurus was deficient in both brown dwarfs (Briceño et al. 2002) and high-mass stars (Walter & Boyd 1991). This contravenes the universality of the IMF, which appears the same in most star-forming regions (Kroupa 2002; Bastian, Covey & Meyer 2010). Recently, the discovery of many brown dwarfs (Luhman 2004; Guieu et al. 2006) has removed the deficit in the low-mass regime.

However, if one extrapolates the IMF to the high-mass regime, there could be up to 40 B-type stars 'missing' from Taurus (Walter & Boyd 1991). Walter & Boyd (1991) proposed that 21 stars in the Cas-Tau OB association were related to Taurus. However, 10 of these candidate members lie outside the field of view in Fig. 1, and presumably have low-mass stars associated with them for which we have no information. To determine the effect of these stars on our results, we first added all 21 candidates to our object list, before running the MST on this, and a list containing only 11 stars that lie within our field of view. In both the cases, the net result is that the B-type stars are even more inversely mass segregated than solar mass stars.

In short, if there are missing B-type stars from our observational sample, we would expect them to simply reinforce our main results. However, we note that in some cases, sampling an IMF to populate a low-number cluster such as Taurus could, in principle, lead to a deficiency in a particular mass of object (Parker & Goodwin 2007).

3.6.5 Incompleteness in the low-mass regime

In Fig. 1, the fields for which the observations are thought to be entirely complete (Luhman et al. 2010; Monin et al. 2010, and references therein) are indicated by the solid lines. Outside these regions, it is possible that surveys of Taurus may have missed objects, particularly low-mass stars and brown dwarfs. Such missing objects may impact upon the results of our MST technique. To qualify the potential effects of missing objects, we have run the MST on the central region only (encompassed by the solid line in Fig. 1). The results are shown in Fig. 6. The most massive objects have a mass segregation ratio $\Lambda_{MSR} = 0.81^{+0.10}_{-0.05}$, which is not as extreme a trough as the $\Lambda_{MSR} = 0.70 \pm 0.10$ found for the whole association. However, in Fig. 1, one can clearly see that many of the most massive stars in the association are located outside of the central region. If the sparsely populated regions in-between the central region and the groups *are* more or less complete, then omitting the outlying regions from the analysis is potentially adding a bias to the results because we are no longer considering the entire star-forming region.

Interestingly, recently Kirk & Myers (2010) studied the subgroups of stars within Taurus and found that the most massive stars in the groups are mass segregated. Kirk & Myers (2010) determined the centre of each subgroup, and then calculated the offset from the centre for each star. They find that the most massive star in each
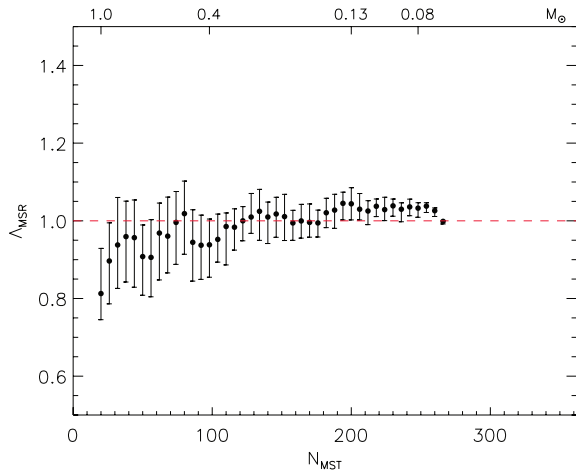
Figure 6. As Fig. 2, but for the central region marked by the black outline in Fig. 1. The dashed line indicates $\Lambda_{\mathrm{MSR}} = 1$, i.e. no mass segregation. We also show the lowest mass within N_{MST} stars on the top axis.

group has an offset which is significantly lower than the median. We also reproduce this result if we calculate Λ_{MSR} on e.g. the L1551 group (Gomez et al. 1993) enclosed by the black outline at the bottom of Fig. 1. For each of the subgroups, we find that the most massive stars are mass segregated. However, the calculated values for Λ_{MSR} are not as robust as those for the whole association due to low-number statistics. We prefer to consider the entire association in our analysis, as the subgroups are interlinked via gas filaments, so star formation must be happening on a global scale.

Additionally, a great deal of observational effort has gone into improving the completeness of the entire association and it may be that the data are more or less complete (e.g. Guieu et al. 2006; Luhman et al. 2010). Furthermore, star formation is recognized to be more prominent in filaments, which have strong CO signatures and high dust extinction (e.g. Palla & Stahler 2002; Schmalzl et al. 2010, and references therein). Indeed, Luhman et al. (2009) show that dust extinction (Dobashi et al. 2005) is strongly correlated with known members, with little evidence of filaments elsewhere, suggesting that the stellar census is complete.

Finally, we note that any theory of star formation in Taurus must reproduce the inverse mass segregation we observe over a large scale *and* the localized mass segregation observed by Kirk & Myers (2010). We will examine this in detail in a forthcoming paper.

3.6.6 Extinction

A further related issue to completeness is the variation of extinction across the cluster. In the most clustered regions, the faintest objects may not be detected due to their being embedded in the gas. As a check, we discarded all objects with an extinction $A_v > 4$ and repeated the analysis. Again, we find no discernible difference to the results.

4 COMPARISON WITH OTHER METHODS AND DATA SETS

In this section, we compare the results of the MST analysis of our Taurus data set with other data sets and methods that have previously been used to analyse the spatial distribution of objects in Taurus.
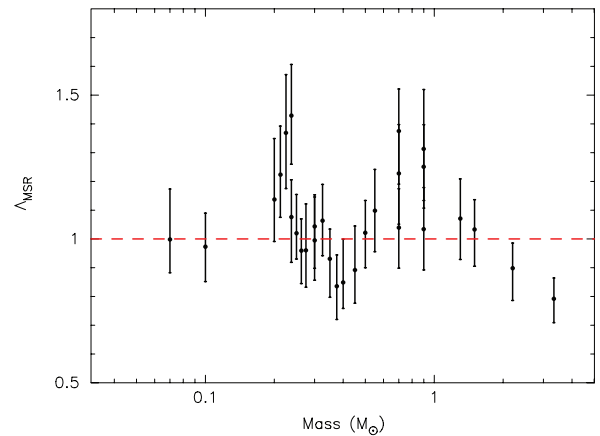

Figure 7. As Fig. 4, but computed with data provided in Luhman et al. (2010). The mass segregation ratio, Λ_{MSR}, is plotted as a function of the most massive object in each subset of 40 stars. The dashed line indicates $\Lambda_{\mathrm{MSR}} = 1$, i.e. no mass segregation.

4.1 Comparison with other data

In a recent work, Luhman et al. (2010) provided a list of 324 members of Taurus for which spectral types could be assigned to each object. From these spectral types, masses were inferred using the isochrones of Siess et al. (2000). As an independent test of our method, we repeat the step MST analysis in Section 3.5 for the objects in Luhman et al. sample and our results are shown in Fig. 7. It should be noted that the subsets of objects lie in slightly different locations to those calculated using our data set in Fig. 4, due to the fact that there are 37 fewer members overall, and objects with similar spectral types are assigned the same masses, causing the 'pile-up' of mass segregation ratios at some mass values. However, in general, the results are very similar to those using our data; the brown dwarfs have $\Lambda_{\mathrm{MSR}} \sim 1$, whereas stars with masses less than $1\,\mathrm{M_{\odot}}$ appear mass segregated with the anomalous feature still prevalent at $0.3\,\mathrm{M_{\odot}}$. The data from Luhman et al. (2010) are also consistent with $\Lambda_{\mathrm{MSR}} = 0.7$ (within the uncertainties) for the most massive objects in Taurus.

4.2 The $\mathcal{R}_{\mathrm{ss}}$ ratio of substellar–stellar objects

Previous studies into the spatial distribution of brown dwarfs in Taurus measured the ratio of brown dwarfs to stars for both the whole cluster and the separate aggregates:

$$\mathcal{R}_{\mathrm{ss}} = \frac{N(0.02 < m/\mathrm{M_{\odot}} \leq 0.08)}{N(0.08 < m/\mathrm{M_{\odot}} \leq 10)}. \qquad (2)$$

This ratio has been calculated for the whole Taurus association (Briceño et al. 2002; Luhman 2004; Guieu et al. 2006) resulting in a range of values depending on the chosen data set. For example, Briceño et al. (2002) find $\mathcal{R}_{\mathrm{ss}} = 0.13 \pm 0.04$, Luhman (2004) finds $\mathcal{R}_{\mathrm{ss}} = 0.18 \pm 0.04$ and Guieu et al. (2006) find $\mathcal{R}_{\mathrm{ss}} = 0.23 \pm 0.04$. Guieu et al. (2006) also applied the $\mathcal{R}_{\mathrm{ss}}$ ratio to the various aggregates and concluded that the brown dwarfs are less abundant (by a factor of ~ 2) compared to stars in the aggregates than for the overall cluster.

An overall cluster value of $\mathcal{R}_{\mathrm{ss}} = 0.23 \pm 0.04$ is consistent with the Trapezium cluster (Briceño et al. 2002), whereas lower values suggest a deficiency in the substellar IMF. However, Luhman (2006) argues that the $\mathcal{R}_{\mathrm{ss}}$ ratio is strongly biased by the assignment

of spectral type to a particular object (as this changes both the numerator and the denominator of equation 2).

A further related problem lies in determining the completeness of the substellar population. For example, if we have 30 brown dwarfs and 220 stars, $\mathcal{R}_{ss} = 0.14$. If a further 10 brown dwarfs are added to the sample, the ratio of substellar to stellar objects becomes $\mathcal{R}_{ss} = 0.18$. In other words, a normal IMF can appear abnormal simply due to the observational incompleteness. Such a change to the sample would not drastically affect the results of the MST technique, unless the majority of the missing brown dwarfs were spatially distributed in a very different fashion to other objects of similar mass in the sample.

4.3 Nearest neighbour distances

In order to minimize the perceived biases associated with the $\mathcal{R}_{ss}$ ratio, Luhman (2006) adopted the nearest neighbour distance as a method of quantifying the spatial distribution of brown dwarfs in Taurus. In this analysis, Luhman (2006) classified objects with spectral type >M6 as brown dwarfs, and objects ≤M6 as stellar objects. To account for the potential incompleteness in the range M2–M6, Luhman (2006) also made a subclassification of stars as ≤M2, and compared objects with >M6 to both ≤M6 and ≤M2.

For each object class, Luhman (2006) determined the distance to the nearest neighbour. He examined the distance from each >M6 (brown dwarf) and ≤M2 (star) to the nearest ≤M2; and the distance from each >M6 (brown dwarf) and ≤M6 (star – second definition) to the nearest ≤M6 – see his fig. 14. We repeat his analysis for the data set used here and our results are shown in Fig. 8.

We agree with the conclusion of Luhman (2006); the distances between brown dwarfs and stars, and stars and stars, do not differ much in our data set. However, there do appear to be subtle variations in the spatial distribution as a function of the mass of the object in Taurus (recall Figs 4 and 7). These differences are not apparent in the nearest neighbour analysis. In Fig. 8, the distributions

of the nearest neighbour distances between any chosen groups of objects are identical. Guieu et al. (2006) find a similar result, and both authors found the distribution of stellar and substellar nearest neighbour distances to be consistent.

We therefore caution against using the mean nearest neighbour distance to define the spatial distribution of brown dwarfs compared to stars in a cluster. If the mass function of Taurus is normal, we would expect there to be 4–5 times as many stars as brown dwarfs in the cluster (Andersen et al. 2008). If we calculate the average nearest neighbour distance between the brown dwarfs in our sample, we obtain a value of 33 arcmin compared to a value of 11 arcmin between stars. However, this technique is biased towards obtaining smaller nearest neighbour distances for stars because there are more of these objects in the cluster than brown dwarfs. Therefore, the stars are more likely to be closer to other stars than the brown dwarfs are to other brown dwarfs.

If we compare the MST length between brown dwarfs to the MST length of random sets of stars, we obtain a (largely) unbiased determination of the spatial distribution of these objects, and we are also able to pick out the subtle differences in the distribution of intermediate-mass stars and the highest mass stars (see Figs 4 and 7).

Finally, we note that other comparisons between the MST technique and nearest neighbour distance also find the MST to be a more robust determination of spatial distribution (Gutermuth et al. 2009).

5 DISCUSSION

We have calculated Λ_{MSR} (Allison et al. 2009) for stellar and substellar objects across the entire Taurus association. We find that the most massive stars in the cluster ($m > 1.2\,M_{\odot}$) are slightly inversely mass segregated with respect to random stars with a trough at $\Lambda_{MSR} = 0.70 \pm 0.10$ ($\Lambda_{MSR} = 1$ indicates no mass segregation). This result is unusual because Orion (often considered to be a 'typical'
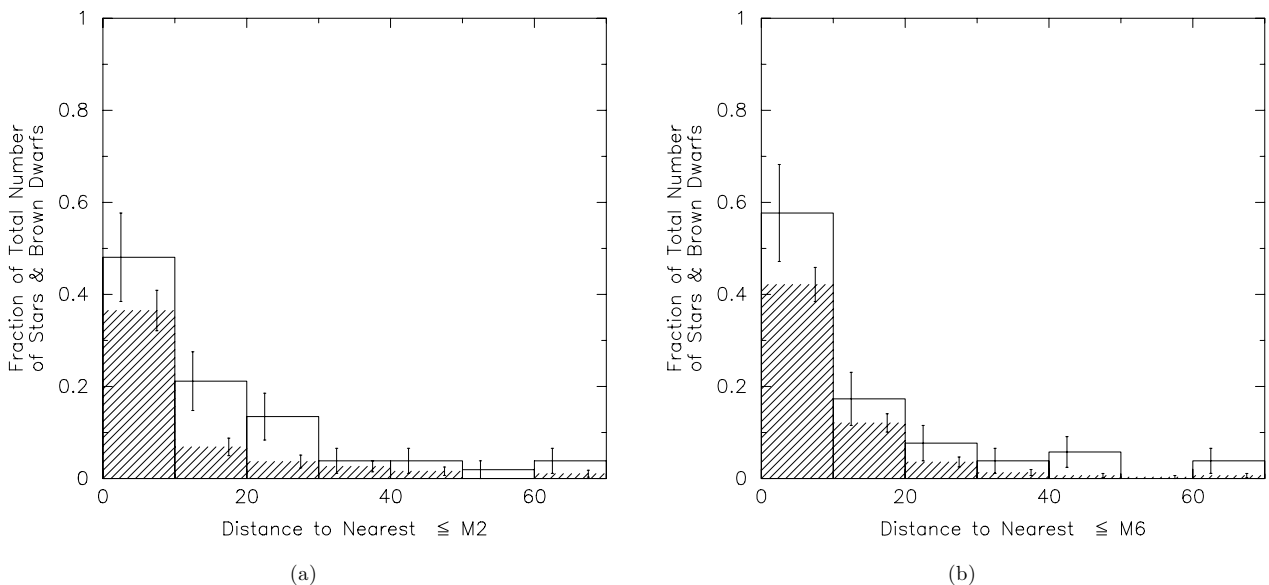

(a)   (b)

Figure 8. The distances to nearest neighbours of stars and brown dwarfs. In panel (a), we show a distribution of the distances to the nearest ≤M2 stars from (i) a >M6 brown dwarf (the open histogram with error bars on the left of each bin) and (ii) a ≤M2 star (the hashed histogram with error bars on the right of each bin). Each histogram is normalized to the total number of >M6 or ≤M2 objects. In panel (b), we show a distribution of the distances to the nearest ≤M6 star from (i) a >M6 brown dwarf (the open histogram with error bars on the left of each bin) and (ii) a ≤M6 star (the hashed histogram with error bars on the right of each bin). Each histogram is normalized to the total number of >M6 or ≤M6 objects.

star cluster) displays mass segregation of the most massive cluster members (independent of the method used to define mass segregation) with little or no mass segregation below $5\,M_\odot$ (Allison et al. 2009). Currently, the only other cluster to have been analysed using the MST method is Trumpler 14, and this cluster is similar to Orion in which it displays prominent mass segregation of the most massive stars ($>10\,M_\odot$; Sana et al. 2010).

If the data are complete, they suggest that brown dwarfs are distributed in a slightly different way to most low-mass stars, although within the uncertainties the two distributions are fairly similar. However, if brown dwarfs form via a different mechanism to low-mass stars (e.g. Reipurth & Clarke 2001; Thies & Kroupa 2007) then the observed difference may be real (however see e.g. Padoan & Nordlund 2002, 2004; Stamatellos, Hubber & Whitworth 2007; Whitworth et al. 2007; Bate 2009; Whitworth et al. 2010, for arguments that their formation is similar to that of low-mass hydrogen-burning stars).

Taking the results of this study at face value leads to the following conclusions.

(i) First, the highest mass stars in Taurus ($m > 1.2\,M_\odot$) are more widely distributed than average.

(ii) Secondly, the brown dwarfs and very low mass stars ($m < 0.15\,M_\odot$) are distributed randomly in the cluster and are not found preferentially either within or outside clumps.

(iii) Thirdly, the intermediate-mass stars ($0.15 < m/M_\odot < 0.7$) are more concentrated than a random selection of stars.

(iv) Finally, stars of $\sim 0.3\,M_\odot$ are an exception to the concentration of intermediate-mass stars, seemingly significantly more widely distributed than stars of even slightly higher or lower masses.

A visual inspection of Figs 1 and 5 does suggest that the first three conclusions are at least plausible, especially that the most massive stars are more sparsely distributed. However, the finding that stars of $\sim 0.3\,M_\odot$ are more sparsely distributed than stars slightly more or less massive ($\Lambda_{\mathrm{MSR}} = 0.8$ compared to 1.25) is rather odd, and we will return to this later.

Taurus is dynamically young and relatively unevolved. The stellar and gas densities are closely related (Gomez et al. 1993; Monin et al. 2010), and stars are still forming with at least 20 pre-stellar cores found in the cluster (Kirk, Ward-Thompson & André 2005). Therefore, at least to some extent, the current positions of the stars follow where they formed. That higher mass stars are found preferentially isolated compared to intermediate-mass stars suggests that they form in different places. This may reflect how cores fragment, or possibly how their masses are distributed. It may be that cores that are close together fragment more forming groups of intermediate-mass stars whilst more isolated cores tend to form fewer, but larger, stars. Alternatively, perhaps each core only produces one or two objects, but that lower mass cores cluster more. (It may be argued that these two are equivalent.) We note that the fragmentation scenario should also produce the localized mass segregation of the subgroups in Taurus as found by Kirk & Myers (2010).

Brown dwarfs may be distributed differently to *all* stars of any mass. The statistical significance of this result is too poor to draw any firm conclusions as the total sample size in Taurus is rather small. But this may suggest that brown dwarfs form as a different population to stars in some way (or that very low mass cores are distributed differently). Strong ejections (e.g. Reipurth & Clarke 2001) would be expected to provide a fairly strong signature of inverse mass segregation (as dynamics would not have enough time to erase much of the signature; Goodwin et al. 2005) and so can probably be excluded as also found by Luhman (2006) (see also Joergens

2006). That brown dwarfs are not found to be associated with higher mass stars suggests that disc fragmentation around larger stars is not the formation mechanism behind most brown dwarfs in Taurus (Stamatellos et al. 2007). We note that gentle liberation from binaries may give a slightly sparser distribution of brown dwarfs when compared to low-mass stars (Goodwin & Whitworth 2007).

It would seem unlikely that stars of $0.3\,M_\odot$ would form or dynamically evolve in a significantly different way to stars of mass 0.2 or $0.4\,M_\odot$. It is far more plausible that this effect is due to incompleteness or errors in the mass determinations of these objects. Indeed the spectral types that are missing, M2–M6, may be incomplete (Guieu et al. 2006; Luhman 2006) *outside* the clumpy regions of the cluster. However, for this result to be an artefact of incompleteness this particular spectral range must be incomplete *inside* the clumps; more M2–M6 stars away from clumpy regions will make the effect more extreme and not less. For this result to be due to incompleteness there must be either (i) more <M2 and >M6 stars in sparser regions to lengthen the MSTs of these types and to lengthen the average MSTs or (ii) more stars of M2–M6 within the clumps.

Finally, we note that if the masses of all objects in Taurus were subject to non-systematically change by up to 30 per cent, then the feature at $0.3\,M_\odot$ may disappear. Further work to better constrain the masses of these objects would obviously be desirable.

We will return to a more detailed theoretical analysis of these results in a future paper.

6 CONCLUSIONS

We have applied the MST method (Allison et al. 2009) to search for mass segregation (both normal and inverse) in the stellar and substellar populations of the Taurus association. To this end, we determine the MST length of the 20 least massive stars and compare this with the MST lengths of random sets of stars. We repeat the procedure for the MST length of the 20 most massive stars. The level of mass segregation is then quantified via the mass segregation ratio (Λ_{MSR}, where $\Lambda_{\mathrm{MSR}} = 1$ corresponds to no mass segregation).

We also apply a new variation of the MST method to compare the MST lengths of subsets of 40 objects to 40 random objects, thereby allowing us to trace the evolution of Λ_{MSR} as a function of object mass. This enables the mass segregation ratio of intermediate-mass objects to be calculated.

We determine Λ_{MSR} for the most massive stars ($m \gtrsim 1.2\,M_\odot$) in Taurus and find them to be slightly inversely mass segregated ($\Lambda_{\mathrm{MSR}} = 0.70 \pm 0.10$), i.e. preferentially located towards the outskirts of the cluster. This is unusual in that other star clusters show mass segregation of the most massive stars (Allison et al. 2009; Sana et al. 2010), although such clusters are more massive, and dense, than Taurus.

We find that the brown dwarfs in Taurus have a mass segregation ratio consistent with no mass segregation, although we find tentative evidence that intermediate-mass stars ($0.15 < m/M_\odot < 0.7$) show slight mass segregation with $\Lambda_{\mathrm{MSR}} = 1.25 \pm 0.15$.

These results suggest that brown dwarfs are distributed randomly in the cluster, whilst intermediate-mass stars are generally concentrated in clumpy regions, and higher mass stars are distributed more widely than average. We note that the observations of stellar and substellar objects in Taurus may be incomplete for spectral types later than M2, and further surveys are desirable in order to determine whether low-mass stars are distributed differently to brown dwarfs. Whilst incompleteness, especially away from the populous well-studied regions, may affect our conclusions for low-mass stars,

it is unlikely that any higher mass stars are missing from the surveys of Taurus and so, unless there is a significant population of low-mass stars away from the known clumps, this result is robust.

Our method avoids the need for the sometimes arbitrary choice of cluster centre necessary in radially dependent searches for mass segregation. It also directly compares the path-length between objects of similar mass and random objects, rather than the nearest neighbour distance between stars and brown dwarfs, or the number ratio of brown dwarfs to stars in a particular region and we consider it to be a more quantitative measure of mass segregation than previous techniques. In a follow-up paper, we will use the MST method to compare models of pre-stellar core fragmentation with the observational data (Parker et al., in preparation).

ACKNOWLEDGMENTS

REFERENCES

Adams J. D., Stauffer J. R., Monet D. G., Skrutskie M. F., Beichman C. A., 2001, AJ, 121, 2053
Allison R. J., Goodwin S. P., Parker R. J., Portegies Zwart S. F., de Grijs R., Kouwenhoven M. B. N., 2009, MNRAS, 395, 1449
Andersen M., Meyer M. R., Greissl J., Aversa A., 2008, ApJ, 683, L183
Bastian N., Covey K. R., Meyer M. R., 2010, ARA&A, 48, 339
Bate M. R., 2009, MNRAS, 392, 590
Briceño C., Hartmann L., Stauffer J., Martin E., 1998, AJ, 115, 2074
Briceño C., Luhman K. L., Hartmann L., Stauffer J. R., Kirkpatrick J. D., 2002, ApJ, 580, 317
Cartwright A., Whitworth A. P., 2004, MNRAS, 348, 589
Dobashi K., Uehara H., Kandori R., Sakurai T., Kaiden M., Umemoto T., Sato F., 2005, PASJ, 57, 1
Gomez M., Hartmann L., Kenyon S. J., Hewitt R., 1993, AJ, 105, 1927
Goodwin S. P., Whitworth A. P., 2007, A&A, 466, 943
Goodwin S. P., Hubber D. A., Moraux E., Whitworth A. P., 2005, Astron. Nachr., 326, 1040
Gouliermis D., Keller S. C., Kontizas M., Kontizas E., Bellas-Velidis I., 2004, A&A, 416, 137
Güdel M. et al., 2007, A&A, 468, 353
Guieu S., Dougados C., Monin J.-L., Magnier E., Martín E. L., 2006, A&A, 446, 485
Gutermuth R. A., Megeath S. T., Myers P. C., Allen L. E., Fazio J. L. P. G. G., 2009, ApJS, 184, 18
Joergens V., 2006, A&A, 448, 655
Kenyon S. J., Hartmann L., 1995, ApJS, 101, 117
Kenyon S. J., Dobrzycka D., Hartmann L., 1994, AJ, 108, 1872
Kenyon S. J., Gómez M., Whitney B. A., 2008, in Reiparth B., ed., Handbook of star forming regions Vol. I, Low Mass Star Formation in the Taurus-Auriga Clouds. Astron. Soc. Pac., San Francisco, p. 40
Kirk H., Myers P. C., 2010, ApJ, preprint (arXiv:1011.1416)
Kirk J. M., Ward-Thompson D., André P., 2005, MNRAS, 360, 1506
Kroupa P., 2002, Sci, 295, 82
Kroupa P., Bouvier J., 2003, MNRAS, 346, 343
Littlefair S. P., Naylor T., Jeffries R. D., Devey C. R., Vine S., 2003, MNRAS, 345, 1205
Luhman K. L., 2000, ApJ, 544, 1044
Luhman K. L., 2004, ApJ, 617, 1216
Luhman K. L., 2006, ApJ, 645, 676
Luhman K. L., Allen P. R., Espaillat C., Hartmann L., Calvet N., 2010, ApJS, 186, 111
Luhman K. L., Briceño C., Stauffer J. R., Hartmann L., Barrado y Navascués D., Caldwell N., 2003, ApJ, 590, 348
Luhman K. L., Mamajek E. E., Allen P. R., Cruz K. L., 2009, ApJ, 703, 399
Monin J.-L. et al., 2010, A&A, 515, 91
Padoan P., Nordlund Å., 2002, ApJ, 576, 870
Padoan P., Nordlund Å., 2004, ApJ, 617, 559
Palla F., Stahler S. W., 2002, ApJ, 581, 1194
Parker R. J., Goodwin S. P., 2007, MNRAS, 380, 1271
Prim R. C., 1957, Bell Syst. Tech. J., 36, 1389
Reipurth B., Clarke C. J., 2001, AJ, 122, 432
Sabbi E. et al., 2008, AJ, 135, 173
Sana H., Momany Y., Gieles M., Carraro G., Beletsky Y., Ivanov V. D., De Silva G., James G., 2010, A&A, 515, 26
Schmalzl M. et al., 2010, ApJ, 725, 1327
Siess L., Dufour E., Forestini M., 2000, A&A, 358, 593
Stamatellos D., Hubber D. A., Whitworth A. P., 2007, MNRAS, 382, L30
Thies I., Kroupa P., 2007, ApJ, 671, 767
Ungerechts H., Thaddeus P., 1987, ApJS, 63, 645
Walter F. M., Boyd W. T., 1991, ApJ, 370, 318
Whitworth A. P., Bate M. R., Nordlund Å., Reipurth B., Zinnecker H., 2007, in Reipurth B., Jewitt D., Keil K., eds, Protostars and Planets V. The Formation of Brown Dwarfs: Theory. Univ. Arizona Press, p. 459
Whitworth A. P., Stamatellos D., Walch S., Kaplan M., Goodwin S., Hubber D., Parker R., 2010, in de Grijs R., Lépine J. R. D., eds, IAU Symp. 266, The Formation of Brown Dwarfs. Cambridge Univ. Press, Cambridge, p. 264

This paper has been typeset from a TEX/LATEX file prepared by the author.